In situ HRTEM of crystallization of nickel-deposited amorphous silicon thin film

Sung Bo Lee[a], Duck-Kyun Choi[a] and Fritz Phillipp[b]
[a]*Department of Ceramic Engineering, Hanyang University, Seoul 133-791, Korea*
[b]*Max-Planck-Institut für Metallforschung, Heisenbergstrasse 3, D-70569 Stuttgart, Germany*

1. Introduction

Bulk amorphous silicon (*a*-Si) crystallizes at about 600-700°C [E.g., 1] and this intrinsic crystallization temperature is lowered by addition of metal impurities, such as Au [2], Al [3], and Sb [4], which form eutectics with Si, and Ni [5-7], which forms various silicides with Si. For the eutectic-forming metals, Radnoczi *et al.* suggested that Au, Sb, and Al dissolved in the *a*-Si film may loosen the covalent bonding in the *a*-Si and make the *a*-Si even unstable, enhancing crystallization [3].

Different from the case of eutectic-forming metals, for the silicide-forming metal, such as Ni, silicides are reported to mediate crystallization [5-7]. Hayzelden and his coworkers [5,6] observed that after $NiSi_2$ precipitates with CaF_2 structure, which have a close lattice match to Si (-0.4 %), form in *a*-Si in the shape of octahedra bounded by eight {111} faces at about 400°C, then at a higher temperature of 500°C, the *c*-Si is epitaxially nucleated on one or more of the $NiSi_2$ {111} surfaces. The $NiSi_2$ precipitates are observed to migrate in the *a*-Si films, leaving *c*-Si needles behind ($NiSi_2$-mediated crystallization) [5,6]. Erokhin *et al.* [7] also observed similar phenomena. They [6,7] suggested that crystallization is enhanced by solid-phase transport of Si through the silicides. However, in a Ni/*a*-Si/*c*-Si layered system, Mohadjeri *et al.* [8] presented another possibility of crystallization mechanism than in the previous results [6,7]: During annealing at various temperatures between 350 and 425°C, nickel monosilicide (NiSi) forms at the Ni/a-Si interface and Ni diffuses toward at the *a*-Si/*c*-Si interface through the *a*-Si layer. Crystallization starts at the *a*-Si/*c*-Si interface, where

the presence of Ni is detected without any certain indication of $NiSi_2$ formation, suggesting that the presence of Ni solutes promotes crystallization.

In this Letter we reinvestigate the effect of Ni on crystallization of *a*-Si in a Ni-deposited *a*-Si thin film by *in situ* high-resolution transmission electron microscopy (HRTEM). During annealing at 550°C in the TEM, crystallization occurs with $NiSi_2$ formation. Nanometer-sized Ni particles are also observed, but crystallization does not occur around them. The dependence of crystallization behavior on the particle types leads to the suggestion that crystallization is promoted by the presence of Ni, not by that of $NiSi_2$.

2. Experimetal Procedure

A Ni-deposited *a*-Si thin film was made in the following way: On Corning 1737 glass, thin 80 nm *a*-Si was deposited by plasma-enhanced chemical vapor deposition (PECVD) at 280°C using Si_2H_6 and H_2 as source gases. A thin 2 nm Ni layer was deposited on the *a*-Si layer on the glass by DC sputtering. Disks of 3 mm diameter were cut from the wafer using a disk cutter for TEM specimen preparation. The disks were mechanically back-thinned to a thickness of about 20 m, and then ion-milled on the glass substrate side at an accelerating voltage of 4 kV using a PIPS. *In situ* observations were made in plan-view at a temperature of 550°C, using the Jeol JEM-ARM1250 at the Max-Planck-Institut für Metallforschung (Stuttgart, Germany) and the Jeol JEM-ARM1300S at the Korea Basic Science Institute (Daejeon, Korea), both of which are operated at 1.25 MeV (0.12 nm point-to-point resolution) and equipped with a side-entry heating stage. The base pressure in the specimen chamber is in the range of 2 - 3 10^{-6} Pa. The heating rate was 20°C/min. Electron current densities at the specimens were in the range of 15 - 20 A/cm^2 during the observations.

3. Results

Figure 1(a) shows a microstructure taken after annealing for 100 min. The measured spacings of three sets of planes are nearly identical to the {220} spacings (1.920 Å) of Si (cubic, *a* = 5.430 Å) or the {220} spacings (1.911 Å) of $NiSi_2$ (cubic, *a* = 5.406 Å) [9]. (Lattice images of Si and $NiSi_2$ are not distinguished from each other in the plan-view observation, because the

silicide with CaF_2 structure has a close lattice match to Si (-0.4 %).) These measured spacings and the intersecting angles between the planes show that the plan-view of Fig. 1(a) is the {111} surface of Si or $NiSi_2$. It is understood in Fig. 1(a) that at this annealing stage (e.g., after annealing for 124 min) the surface Ni layer reacts with the underlying *a*-Si to form $NiSi_2$, as for Ni-deposited *c*-Si [10-15].It cannot be excluded in Fig. 1(a) that a very thin layer *c*-Si forms below the $NiSi_2$ layer. After prolonged annealing (e.g., for 252 min), as shown in Fig. 1(b), the {111} zone becomes to have larger interplanar spacings. Such spacings are not produced by the Si{220} reflections corresponding to the spacings of 1.920 Å, but seem to arise from the forbidden 1/3 {422}reflections of Si corresponding to the spacings of 3.327 Å. The forbidden reflections are attributed to {111} twins and stacking faults of *c*-Si [1]. Thus, Fig. 1(b) clearly shows that *a*-Si crystallizes below the $NiSi_2$ layer and that we are observing the plan-view of the overlap of the $NiSi_2${111} and *c*-Si{111} layers.

In addition to the $NiSi_2$, nanometer-sized Ni particles (cubic, Ni with 0-18 at% Si, a = 3.525-3.515 Å) [16] are observed, as shown in Fig. 2. The Ni particles shown in Figs. 2(a) and (b) show their [110] zone axis being parallel to the beam direction without tilting, and their sizes are in the range of 3 - 4 nm in equivalent-sphere diameter. The measured interplanar spacings indicated in Fig. 2 correspond to the {111} spacings (2.035 Å) of Ni. Some particles are single crystals revealing {111} and {100} surface facets arising from truncated octahedral shape, as shown in Fig. 2(a), and the others are observed to contain more than one twin boundaries (multiply twinned), as represented in Fig. 2(b). The particle in Fig. 2(b) also reveals flat {111} surfaces, but faceting is not so distinct as compared with Fig. 2(a). It is well known that small nanoparticles of f.c.c. metals take a structure of the decahedral or icosahedral multiply twinned particles (MTPs) [17-19]. Figure 2(b) represents a decahedral MTP viewed along the five-fold axis in the [110] direction. Different from the case of the $NiSi_2$, crystallization does not occur around the Ni particles.

4. Discussion

Below the eutectic temperature of 993°C, $NiSi_2$ is in equilibrium with Si

[20], and actually, it is reported to exist at the Ni/*c*-Si interface [10-15]. The formation of the Ni particles in the present study may be attributed to heat evolution effect by electron-beam during the observations. Because of the poor thermal conductivity of the *a*-Si layer and the glass substrate, the heat generated by electron beam is not expected to be efficiently dissipated. In this situation, the formation of $NiSi_2$ will be prevented, because it is an exothermic reaction [21]. Presently, it is not clear from Fig. 2 whether they are nonreacted Ni or Ni solid solution (containing up to 18 at% Si). However, as mentioned above, the thin surface Ni layer tends to react with Si to form equilibrium $NiSi_2$phase. Even with prolonged annealing (e.g., 206 min in Fig. 2(b)), the particles remain untransformed, which indicates that Ni does not diffuse into *a*-Si, and therefore, we can deduce that they are nonreacted Ni.

Nickel is observed to be the dominant diffusing species in the formation of $NiSi_2$ [22], and in a Ni/*a*-Si interface, Ni atoms will diffuse into the *a*-Si layer to form $NiSi_2$. During the formation of $NiSi_2$, a small amount of Ni atoms may not be incorporated into the formed $NiSi_2$. As in the case of the eutectic-forming metals suggested by Radnoczi *et al.* [3], such *free* Ni atoms can diffuse into the *a*-Si layer, contributing to crystallization. Such possibility can be found in the observation of Mohadjeri *et al.* [8], which shows that Ni diffuses through the *a*-Si layer toward *a*-Si/*c*-Si interface and the presence of Ni enhances crystallization at the interface. Such Ni solute effect also explains why crystallization is not observed around the Ni nanoparticles: Around them, different from the $NiSi_2$, the Ni diffusion into the *a*-Si is prevented, and concomitantly, crystallization is not expected to occur.

5. Concluding Remarks

To conclude, we have shown through *in situ* HRTEM that the $NiSi_2$ and Ni particles form during annealing at 550°C in the TEM. The Ni particles are single crystalline or multiply twinned. Crystallization occurs around the $NiSi_2$ precipitates, but is forbidden around the Ni particles. These results strongly appear to indicate that crystallization is promoted not by the presence of $NiSi_2$, but by that of Ni.

This work was financially supported by Korea Research Foundation Grant (KRF-2004-005-D00167) and the Alexander von Humboldt Foundation.

References

[1] J. L. Batstone, Phil. Mag. A **67**, 51 (1993).
[2] L. Hultman, A. Robertsson, H. T. G. Hentzell, I. Engström, and P. A. Psaras, J. Appl. Phys. **62**, 3647 (1987).
[3] G. Radnoczi, A. Robertsson, H. T. G. Hentzell, S. F. Gong, and M.-A. Hasan, J. Appl. Phys. **69**, 6394 (1991).
[4] S. F. Gong, H. T. G. Hentzell, A. E. Robertsson, L. Hultman, S. E. Hörnström, and G. Radnoczi, J. Appl. Phys. **62**, 3726 (1987).
[5] C. Hayzelden, J. L. Batstone, and R. C. Cammarata, Appl. Phys. Lett. **60**, 225 (1992).
[6] C. Hayzelden and J. L. Batstone, J. Appl. Phys. **73**, 8279 (1993).
[7] Yu. N. Erokhin, R. Grötzschel, S. R. Oktyabrsky, S. Roorda, W. Sinke, and A. F. Vyatkin, Mater. Sci. Eng. B **12**, 103 (1992).
[8] B. Mohadjeri, J. Linnros, B. G. Svensson, and M. Östling, Phys. Rev. Lett. **68**, 1872 (1992).
[9] K. Schubert and H. Pfisterer, Z. Metallkd. **41**, 433 (1950).
[10] K. C. R. Chiu, J. M. Poate, J. E. Rowe, T. T. Sheng, and A. G. Cullis, Appl. Phys. Lett. **38**, 988 (1981).
[11] F. Föll, P. S. Ho, and K. N. Tu, J. Appl. Phys. **52**, 250 (1981).
[12] R. T. Tung, J. M. Gibson, and J. M. Poate, Phys. Rev. Lett. **50**, 429 (1983).
[13] R. T. Tung, S. Nakahara, and T. Boone, Appl. Phys. Lett. **46**, 895 (1985).
[14] J. L. Batstone, J. M. Gibson, R. T. Tung, and A. F. J. Levi, Appl. Phys. Lett. **52**, 828 (1988).
[15] J. M. Gibson and J. L. Batstone, Surf. Sci. **208**, 317 (1989).
[16] W. Klement, Jr., Can. J. Phys. **40**, 1397 (1962).
[17] S. Ino, J. Phys. Soc. Jpn. **27**, 941 (1969).
[18] A. Howie and L. D. Marks, Phil. Mag. A **49**, 81 (1984).
[19] H. Hofmeister, *Encyclopedia of Nanoscience and Nanotechnology, vol. 3*, edited by H. S. Nalwa (American Scientific Publishers, Stevenson Ranch, CA, 2004), pp. 431-452.
[20] *Binary Alloy Phase Diagrams* (2nd *Edition*), *vol. 3*, edited by T. B. Massalski (ASM International, Materials Park, OH, 1990), p. 2859.

[21] M. E. Schlesinger, Chem. Rev. **90**, 607 (1990).
[22] F. d'Heurle, S. Petersson, L. Stolt, and B. Strizker, J. Appl. Phys. **53**, 5678 (1982).

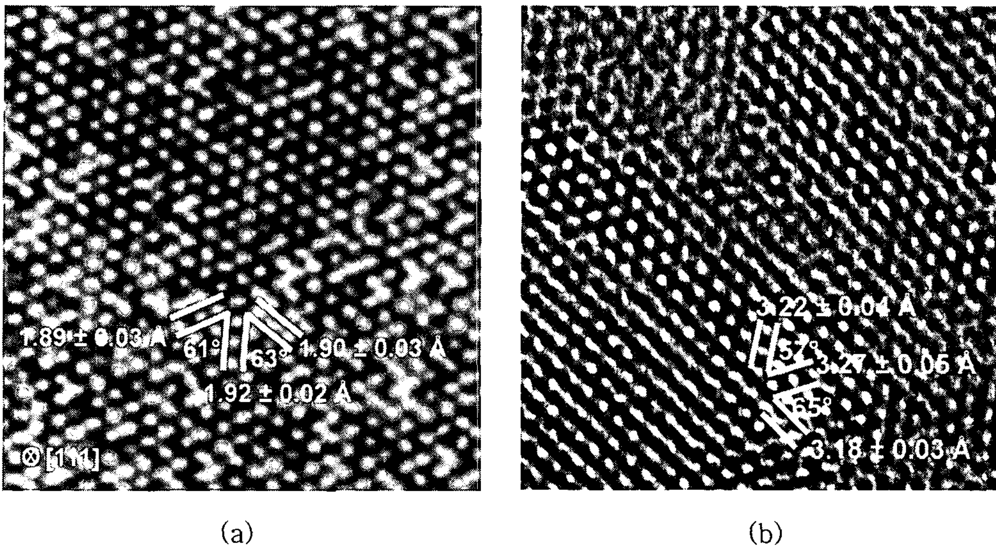

Fig. 1. (a) High-resolution TEM image showing the {111} surface of $NiSi_2$ after annealing at 550°C for 124 min. (b) Plan-view HRTEM image of the $NiSi_2$/*c*-Si {111} interface after annealing for 252 min.

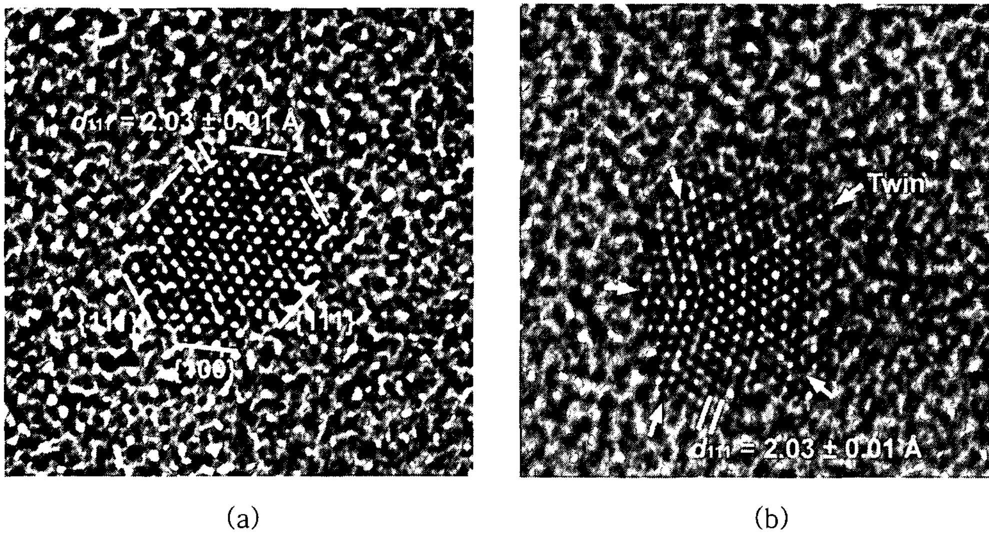

Fig. 2. High-resolution TEM images showing Ni nanoparticles (a) after annealing for 26 min and (b) after annealing for 206 min. In (b), the white arrows show the position of twin boundaries.